

EXPERIMENTAL RESEARCH OF GRAVITATIONAL INSTABILITY AND TURBULIZATION OF FLOW AT THE NOBLE GASES INTERFACE

A. M. Vasilenko, O. V. Buryakov, V. F. Kuropatenko,
V. I. Olkhovskaya, V. P. Ratnikov, V. G. Jakovlev

INTRODUCTION

A special type of turbulence — gravitational turbulence appears at the interface of media having different densities under nonstationary motion because of Taylor instability [1]. This phenomenon takes place, for example, when nonstationary shockwaves pass through nonhomogeneous media.

Theoretical description of the development of small interface perturbations is of no difficulty but in the process of experimental work it came out [2-4], that the growth of finite perturbations, comparable with the wave length, leads to the distortion of their initial form and complicates the analytical examination of this problem [5].

Gravitational turbulent mixing theoretical research made by Belyenkii and Fradkin [6] and some other authors [7-9] is of semi-empirical character. In some works [10-13] gravitational instability numerical research on the ground of Euler nonstationary equations with two spatial variables was carried out.

Experimentally this problem is also poorly investigated. There are few works [14-16] devoted to this question.

The aim of this work is the experimental research of turbulization process of interface perturbations for gases having different densities under the influence of the strong decelerating shockwave under the condition of essential compressibility of initial substance.

The noble gases choice was made in terms of the equality of their adiabatic compressibility. This sufficiently simplifies the experimental analysis.

I. EXPERIMENTAL METHOD

1.1 The Description of the Experiment

The experiments were carried out in the electromagnetic shock tube which is shown in Fig. 1.1. Shock tube frame is made of textolite plates in the form of compartments of different length and purpose. This allows change to not only the total tube length, but also the compartment's position.

Shock tube channel with the cross section of $100 \times 100 \text{ mm}^2$ was partitioned off at the joints by two nitrocellulose diaphragms, 0.4 mm thick, into three compartments filled with various noble gases, as shown in Fig. 1.1.

Such a system of gas layers was subjected to the action of decelerating shockwave. As a result, this caused the state of gravitational instability at the second interface, between Krypton and Helium, in accordance with Taylor criterion [1]. Acceleration at the interface was created by unloading wave defining the flow deceleration. The use of noble gases permitted retention of the initial gas density ratio after the rupture disintegration at the stable interface. The first interface was stable and served for shock-wave intensification in order to create necessary conditions for rapid nitrocellulose diaphragm destruction. These conditions were considered to be satisfied in case the temperature of one of the gases at the interface exceeded nitrocellulose flash temperature.

At the second interface, sinusoidal perturbations were artificially set on lateral sides of the sectional aluminum frame then the nitrocellulose diaphragm was fixed between the sinusoidally preformed frame sections. The profile on the frame is formed by conjugate circle arcs, which is a quite satisfactory approximation to the sinusoidal profile. To avoid significant distortion of set perturbation form on the frame, because of film tension, it was fixed to fifteen nichrome wires 0.12 mm thick, stretched along the profile generator.

In experiments the development of three initial perturbations was examined, namely: $\alpha_0 = 1 \text{ mm}$, $\lambda = 25 \text{ mm}$, $\alpha_0 = 1 \text{ mm}$, $\lambda = 50 \text{ mm}$, $\alpha_0 = 2.5$

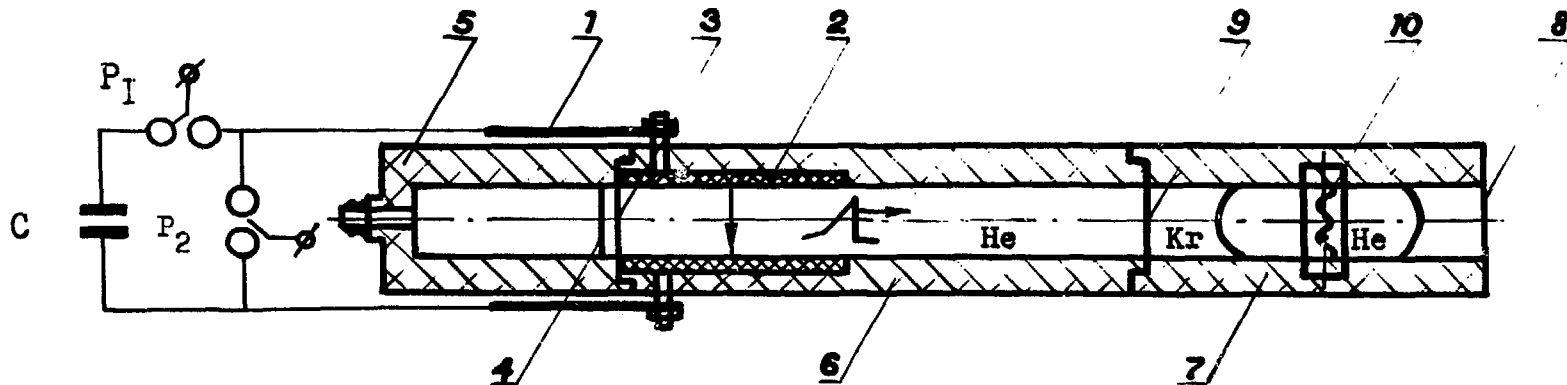


Fig. 1.1 Schematic representation of the electromagnetic shock tube. C - capacitor bank; P_1 , commutative discharger; P_2 , short-circuiting discharger; 1, collector busbar; 2, accelerating electrode; 3, additional diaphragm; 4, principal diaphragm; 5, vacuum compartment; 6, discharge compartment; 7, measuring compartment; 8, diaphragm; 9, joint for thin film mounting; 10, joint in the measuring compartment for the mounting of the frame with a film.

mm, $\lambda = 50$ mm. (α_0 - initial amplitude, λ - wave length). Recording of the perturbations development was carried out by means of a shadow device IAB-451 optically coordinated with two SFR cameras operating in the mode of stop-motion photography and photochronography.

1.2 Main Characteristics of the Electromagnetic Shock Tube

Shock-wave generation was obtained as a result of the discharge of a capacitor bank consisting of 90 capacitors of IS-6.65-20 type. Total inductance of the electromagnetic shock tube circuit equals 223 nH. The electromagnetic shock tube is equipped with a short-circuiting discharger P_2 (see Fig. 1.1). This permits formation of single pulses of the discharge current.

The distinctive feature of the given electromagnetic shock tube [17-19] is a vacuum compartment (5 in Fig. 1.1) which forms the flow behind the front of a rather long shock wave. The front is not distorted by the secondary shock wave. The secondary shock wave appears in the electromagnetic shock tube when forming a single discharge current impulse because of oscillation of a vacuum region formed when the flow layer separates from the shock tube "bottom" under the influence of the intrinsic discharge magnetic field. The flow, forming in the electromagnetic shock tube, is analogous under such conditions to the flow forming in the automodel problem about the short-term shock upon a free gas surface [20]. The flow forming is characterized by the limiting value of shock wave deceleration for the given conditions of experiments.

The vacuum compartment is separated from the shock-tube channel by two thin mylar diaphragms destroyed at the discharge current initial stage.

The first diaphragm had five thin strips of an aluminum foil; each was 2 mm wide and 10 mm thick. They were needed for the electric breakdown between electromagnetic shock-tube accelerating electrodes.

1.3 Calculations for the flow in the electromagnetic shock tube were carried out in accordance with the program "VOLNA" (WAVE) which is intended for mathematic modeling of one-dimensional unsteady motions of compressible ideal media [21].

Physical model realized in the program VOLNA is based on partial differential equations which are a consequence of laws of conservation of mass, momentum, and energy in the Lagrangian coordinate system.

In a common case a domain, where the solution must be found, consists of several regions, each characterized by its own equation of state, by its own speed, and by its thermodynamic parameters set at the initial moment of time. Regions are separated from each other by interfaces or vacuum gaps. Boundary conditions are pistons where either speed or initial pressure is set. Nonuniform differential method is used for numerically integrating of set of equations for a given physical model. This method permits tracing the following elements and features:

1. Smooth solutions.
2. Strong, weak and contact ruptures.
3. Phase transformation front — strong or weak rupture on the surface at which the matter phase state changes.
4. Arbitrary rupture disintegration.
5. Strong rupture emergence out of the initially smooth solution.
6. Interaction of strong rupture with initially smooth solution.

To determine the flow parameters at the strong rupture front, the Hugoniot relation is solved in common with the equation for the changing values of velocity along the rupture surface. The equation is of the following form:

$$\frac{d[P]}{dt} + \frac{C^2}{W} \cdot \frac{d[U]}{dt} + A = 0,$$

where:

$$A = \frac{(\alpha - 1) U + V + C^2}{U} + \frac{C_+^2 - W^2 \alpha (r^{\alpha-1})}{W} \cdot \frac{\delta P}{\delta t} + \frac{C^2}{W} \cdot \frac{dU}{dt}. \quad (1.1)$$

Where [P], U represent sudden changes of pressure and velocity on the surface of strong rupture; C is the sound speed; W is the mass velocity of the strong rupture surface; α is the problem symmetry index; r is a spatial coordinate; t is the time. Values with the mark "-" denote the state

"before", and values with the mark "+" denote the state behind the rupture surface.

For the velocity of the shock wave, W , this equation will have the following form:

$$\frac{dW}{dt} + \frac{1}{[U]} \left[\left(\frac{C_+^2}{W} + W \right) \frac{d[U]}{dt} + A \right] = 0 \quad (1.2)$$

Nonuniform differential method realized in WOLNA program uses a regular difference grid for the regions of integrating with smooth solutions and "blurred" features, and also uses a feature refining the grid which is superposed on the regular grid.

Difference schemes included in the nonuniform differential method are obvious and have the first order of approximation in time, and the second order in space on the uniform grid.

In a given case, the impulse of pressure is set on the left gas boundary which corresponds to the beginning of the shock tube. The impulse form is defined by the first semiperiod of the current discharge.

$$P = \begin{cases} P^* \exp(-2t/\tau) \cdot \sin^2 2\pi t/T \text{ npu} & 0 \leq t \leq \frac{T}{2}, \\ 0 & \text{npu} t > \frac{T}{2} \end{cases} \quad (1.3)$$

where:

P^* = parameter which corresponds to effective pressure of the magnetic piston;

T = 75 ms — the period of the bankery discharge;

τ = 78 ms — parameter which characterizes the electric discharge attenuation.

In the calculations according to the WOLNA program, P^* was selected proceeding from the condition of reaching the coordinate $X = 1993$ mm by the shock wave front at $\tau = 522 \mu\text{s}$. We could observe this front in the experiments with helium atmosphere.

P^* was obtained as a result of few calculations for various P which, following interpolation, equaled 140.2 bar.

It is worth mentioning that the flow description with due regard for the secondary shock wave is possible in case of substituting the condition of stopping this boundary ($V = 0$) for the boundary condition on the left gas boundary after terminating the action of the impulse of pressure.

At this moment the secondary shock wave is being formed considering that it corresponded to the left gas boundary which collided with the vacuum compartment "bottom."

Usually, such a procedure was not used because, in this experiment, the process of interaction of the secondary shock wave with the interface was not studied.

The calculations of flow for the description of the gases gravitational instability experiments were carried out in accordance with the specific scheme of gas disposal in the shock-tube channel (see Table 1.1).

TABLE 1.1

N	Gas	γ	ρ g/cm ³	Interface Coordinate mm
1	Helium	1.63	1.6 · 10 ⁻⁴	1087
2	Krypton	1.689	3.364 · 10 ⁻³	1327
3	Helium	1.63	1.6 · 10 ⁻⁴	2500

In the Table: γ — Poisson adiabatic index,
 ρ — gas density.

Gas parameters were determined according to table data [22] and were computed at the experimental conditions. Average atmospheric pressure of gases was 0.984 bar.

Confidence of the results of calculations of the flow in the electromagnetic shock tube is shown in X, t-diagram, Fig. 1.2, where the comparison of the trajectory of the shock-wave front movement with experimental results was carried out. Standard deviation of experimental points from the computed curve was equal to 1.2%. This is in the range of the experimental data scattering.

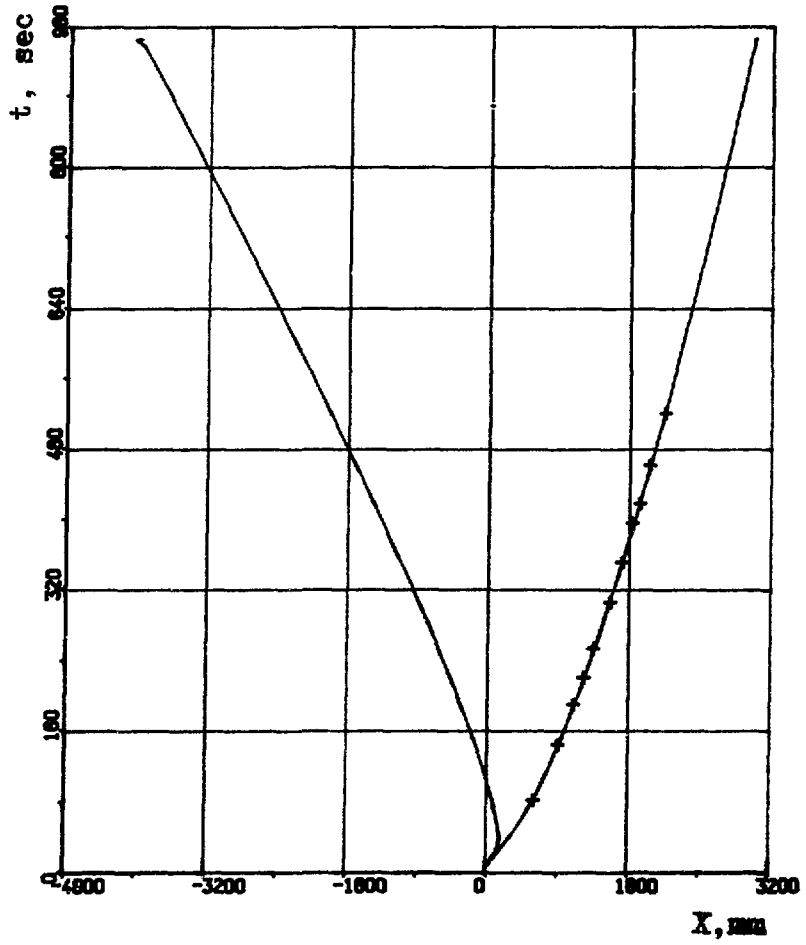


Fig. 1.2 X, t - diagram of the flow in the shock-tube channel in helium atmosphere, - - calculations, + - experiment.

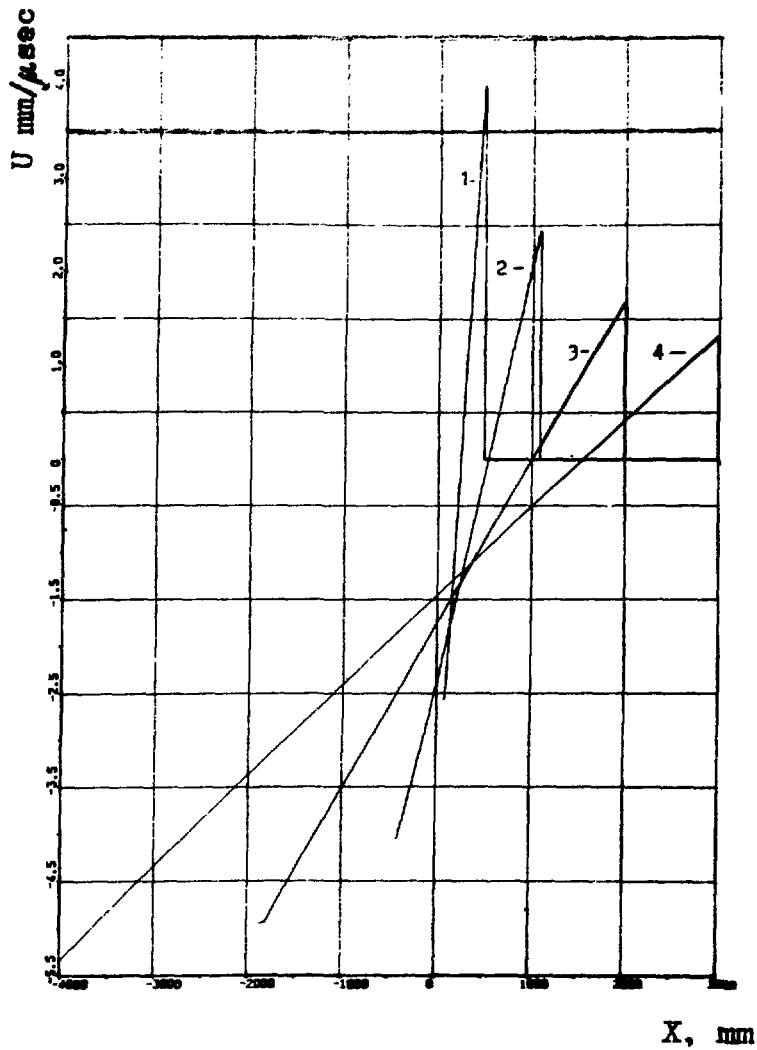


Fig. 1.3 He velocity profiles in the shock tube channel at different moments of time. 1 - 80 μ sec, 2 - 283.9 μ sec, 3 - 522 μ sec, 4 - 946.6 μ sec.

The current layer shift, caused by the discharge's magnetic field and determined by accelerating electrodes erosion, equals 140 mm. This satisfactorily agrees with the computed shift of 150.9 mm on the left gas boundary.

Gas mass velocity profiles shown in Fig. 1.3 have linear form that demonstrates the approaching of flow to the regime which is close to automodel flow in the problem about short-term shock upon the free gas surface.

2. EXPERIMENTAL RESULTS

2.1 Preliminary analysis of physical conditions at the interface was carried out on the basis of the results of one-dimensional gas flow calculations in the electromagnetic shock tube. Just after the rupture disintegration, the pressure at the interface was $P = 3.687$ bar and the velocity of the shock wave falling upon the interface was $W_1 = 0.8114$ mm/ms. Initial mass velocity of gases was $V_0 = 0.94$ mm/ μ s; gas density ratio was 13.75. Breaking distance connected with the unloading wave influence was determined by the formula

$$S = U_0 \hat{t} - \hat{x}, \quad (2.1)$$

where: \hat{t} - time with respect to the moment when the shock wave reaches the interface;
 \hat{x} - distance passed by the interface with respect to the initial position.

Maximum value of the interface deceleration is $g = 10^6$ m/s². By the end of the boundary observation, at the time $t = 1151$ μ s, gas pressure decreases to 2.07 bar, and velocity to 0.487 mm/ μ s.

2.2 The process of the development of the interface gravitational instability and gas turbulent mixing can be conditionally divided into three stages: regular, transitional and turbulent. The regular stage includes the stage of the exponential growth of perturbations in accordance with the linear theory (see [1]) and nonlinear stage, where

deceleration of perturbations growth and the distortion of their form take place, but spatial structure of perturbations is not distorted.

In the transitional stage the distortion of perturbations spatial structure takes place and the regions of flow vorticity arise.

In the turbulent stage intensive initial substance mixing takes place. The experimental results have been analyzed in accordance with such a classification of the stages of the interface instability development. The shadow photographs of the experiments are presented in Fig. 2.1 - 2.3.

2.3 The regular stage was revealed when comparing the experimental results with analytical solution which was obtained by one of the authors for the case of ideal fluids under condition of successive influence of shock and permanent accelerations upon the interface similar to how it happens in the experiment. The development from infinitesimally small perturbations is described by the following equations [23]

$$\frac{d^2 \alpha(t)}{dt^2} = A \kappa g \quad (2.2)$$

with initial conditions:

where $A = \frac{\rho_2 - \rho_1}{\rho_2 + \rho_1}$ - Atwood number,

ρ_2, ρ_1 - heavy and light liquids densities, respectively;

$$\kappa = \frac{2\pi}{\lambda} \quad (2.3)$$

Solution has the following form:

$$\alpha = \alpha_0 \left[\cosh wt - (U_0/W) \cdot \sinh wt \right],$$

where

$$w = \sqrt{Ag\kappa}; \quad W = \sqrt{g/A\kappa}$$

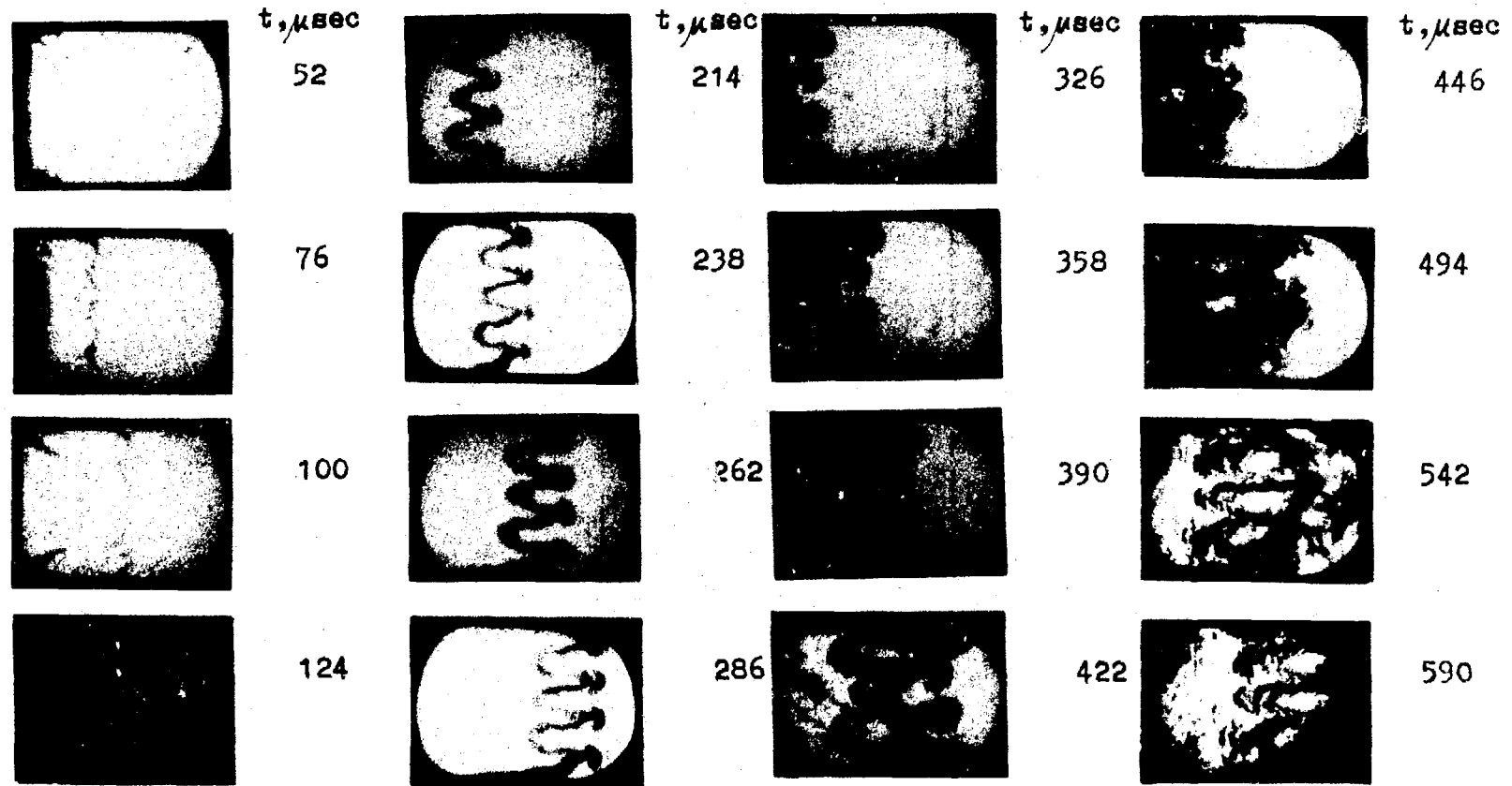


Fig. 2.1 Perturbation development at Kr - He interface with the initial perturbation $\alpha_0 = 1.0$ mm, $\lambda = 25$ mm.

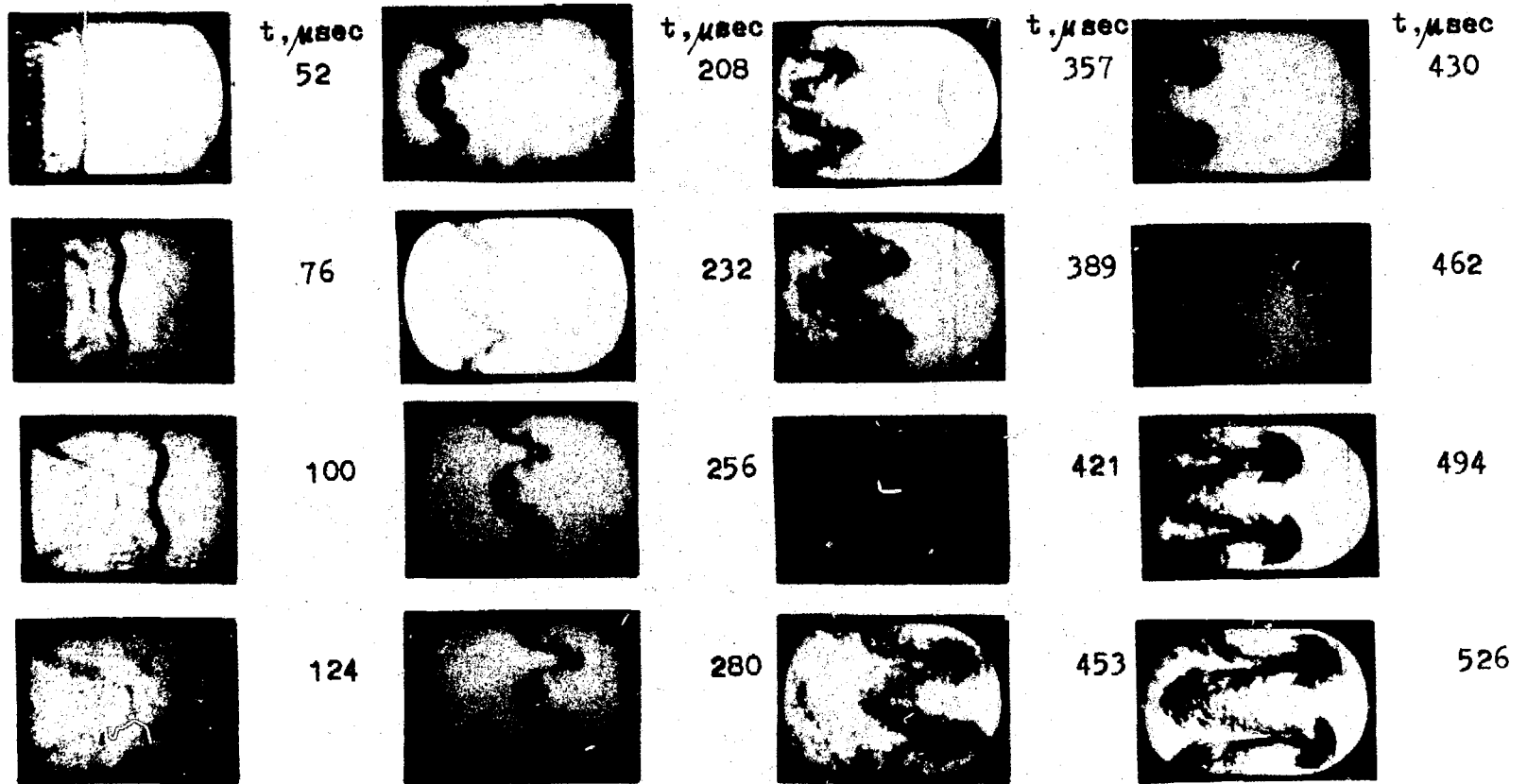


Fig. 2.2 Perturbation development at Kr - He interface with the initial perturbations $\alpha_0 = 1.0$ mm, $\lambda = 50$ mm.

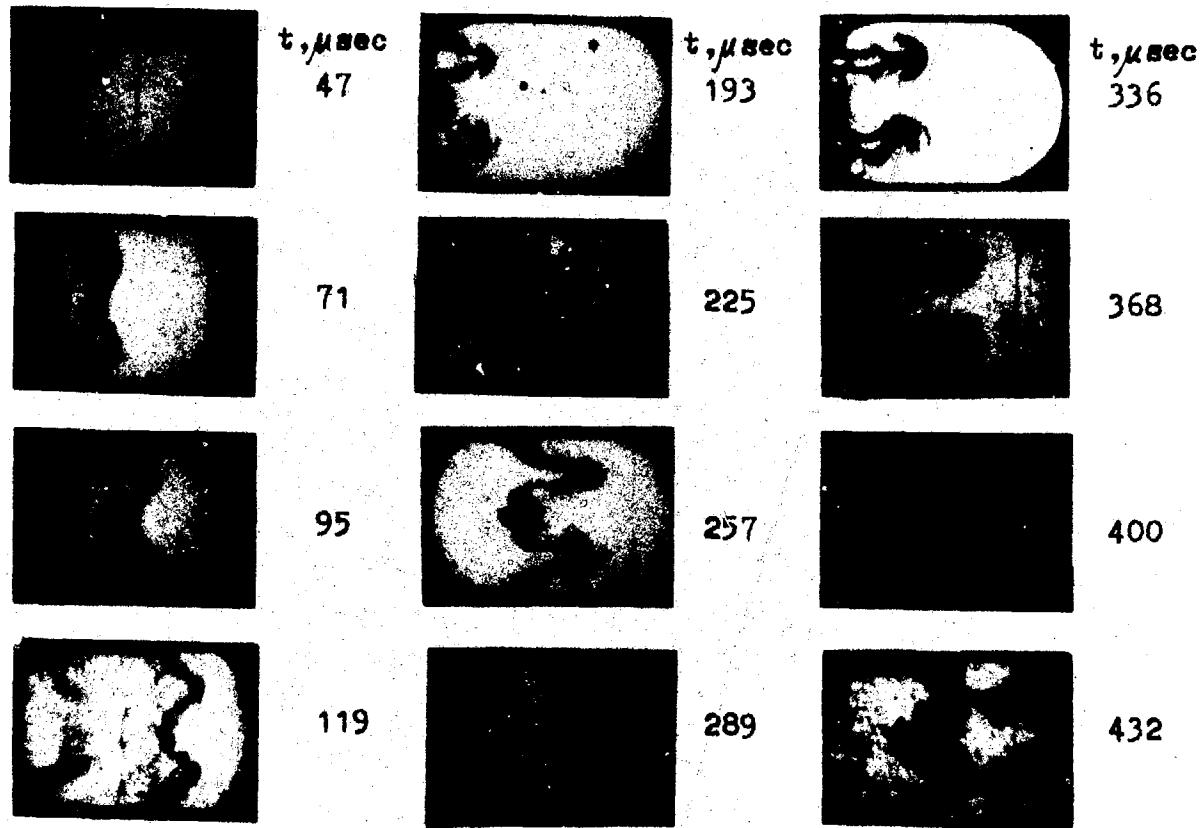


Fig. 2.3 Perturbation development at Kr - He interface with the initial perturbation $\alpha_0 = 2.5$ mm, $\lambda = 50$ mm.

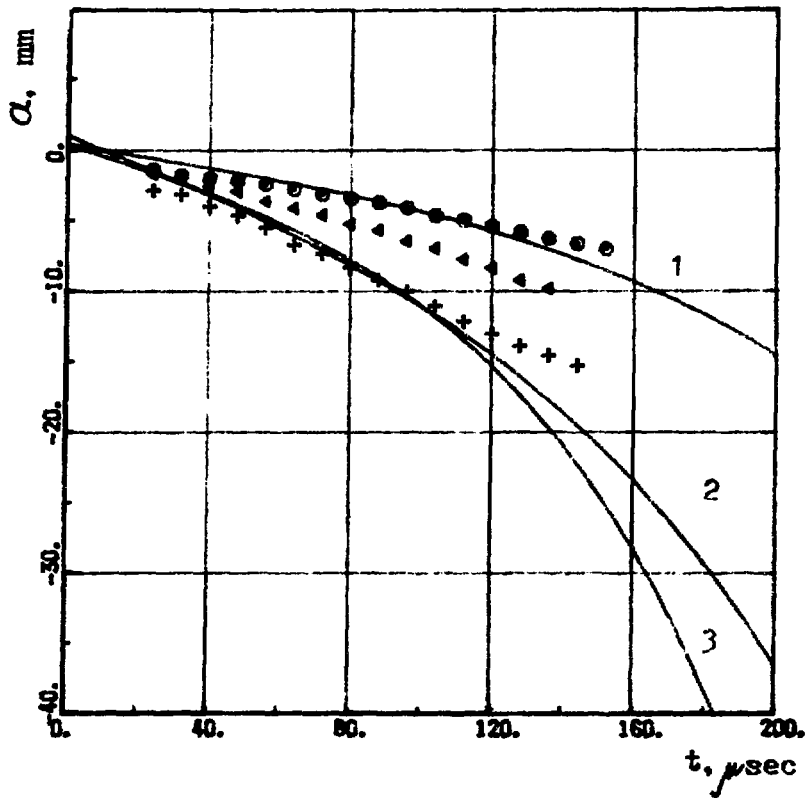


Fig. 2.4 The development of the perturbation amplitudes at the gas interface in the regular stage.

o - $\alpha_0 = 1.0 \text{ mm}$, $\lambda = 50 \text{ mm}$;

\blacktriangleright - $\alpha_0 = 1.0 \text{ mm}$, $\lambda = 25 \text{ mm}$;

+ - $\alpha_0 = 2.5 \text{ mm}$, $\lambda = 50 \text{ mm}$;

1,2,3, - linear impulse theory for perturbations o, \blacktriangleright , + accordingly.

Taking into account the change of the initial perturbation amplitude because of the gas compressibility [24] the solution has the following form:

$$\alpha(t) = \frac{\alpha_0}{2} \left[1 + \left(1 - \frac{U_0}{W_1} \right) \right] \left[\cosh wt - \frac{U_0}{W} \sinh wt \right] \quad (2.4)$$

where: W_1 is the shock wave front velocity before incidence upon the interface.

The gravitational instability development at the process initial stage reveals linear dependence of the perturbations amplitude on time up to the moment $t \sim 130 \mu s$, which is characteristic of the interface shock acceleration [23] and is connected with small role of quasi-stationary acceleration at the initial stage.

Comparison of experimental results with analytical solution (Eq. 2.4) gives every reason to consider that up to the amount $t^* \approx 130 \mu s$ for perturbation with $\lambda = 50 \text{ mm}$ and up to the moment $t^* \approx 30 \mu s$ for perturbations with $\lambda = 25 \text{ mm}$, in the range of 10%-deflection satisfactory agreement of linear impulse theory with experiment is observed. It is worth mentioning that the perturbations amplitude is 5-6 times the initial one. Earlier divergence of the experiment with theory for the perturbations with $\lambda = 25 \text{ mm}$ is explained by evident distortion of sinusoidal profile because of a less number of frame wires per perturbation wave length. As can be seen in the photos 2.1 and 2.2, the influence of these wires upon the process of instability development is not observed. Their indirect influence reveals itself in the distortion of more wide helium jets for the perturbation with $\alpha_0/\lambda = 0.05$ (see Fig. 2.3), which is caused, perhaps, by the nonsmooth character of the initial perturbation form.

Thus, taking into account the satisfactory agreement of experimental results with analytical solution at the considerable period of development up to t^* we can ascertain the satisfactory preparation of experiments. We also can assert that the use of the nitrofilm $0.4 \mu m$ thick does not influence the instability development significantly relative to the process

as a whole, because the systematic distortion of experimental results could have been expected, especially in the initial stage of this phenomenon because of additional film mass involved in the motion. Because of these arguments, any possible doubts concerning the experimental results confidence at later stages of the instability development have no grounds.

2.4 Further development of perturbations leads to distortion of their sinusoidal profiles and to the forming of narrow krypton jets and wider helium jets. The profile distortion begins approximately with t^* , that agrees with the value of W^{-1} , which characterizes the application limit of the linear theory.

At this stage of the perturbation development it is revealed as the result of the asymmetry of gravitational instability, which is characterized by a deeper penetration of krypton jets into helium in comparison with helium jets, penetrating into krypton.

The nonlinear stage of the perturbation development is accompanied by the appearance of vortex regions at the top of krypton jets. The appearance of the vortex regions means the occurrence of a new factor, which did not take place earlier as well as the destruction of the initial spatial structure of perturbation and the transition to the flow turbulization. The flow turbulization in the perturbation zone is accompanied by increasing krypton jet instability that is revealed in their tortuosity. Increasing vortices lead to their closing up with the neighbor ones. That, in its turn, leads to the chaotic state of the flow and to formation of a zone with a complex flow picture on the part of helium. This gas mixing zone can be interpreted, probably, as the zone of the gas turbulent mixing. Full value of this mixing zone reaches 100 mm.

By this time, while observing the interface in a direction, perpendicular relative to the generator of the sinusoidal profile, it was observed that there developed sufficiently significant distortions of perturbation zone front. This demonstrates the destruction of the initial two-dimensional perturbation structure.

Penetration of helium into krypton evolves in the form of wide jets, which are analogous to bubbles in Lewis' experiments [2]. Periodical structures present do not disintegrate even at late times in observing this

phenomena ($\hat{t} \approx 600 \mu\text{s}$, $S = 140 \text{ mm}$). However, the boundaries of helium jets are blurred by a low-scale turbulence which reaches a mean scale of $\approx 40 \text{ mm}$ at $\hat{t} = 500 \mu\text{s}$. Meanwhile, development of the low-scale turbulence displays evident signs of dependence upon an initial perturbation amplitude. When the initial amplitude rises, blurring of jet interface is decreased.

The development of gas jet flow (krypton jets are especially significant), which proceeds from the laminar flow through the transient one to turbulent flow, is analogous to turbulization of free turbulent jets [25]. It demonstrates the commonality of some features of gravitational and shearing turbulences, namely: chaotic state, periodic structure, component mixing, independence from initial conditions.

One can see the nearly periodic regions where krypton jet boundaries are distorted. Chaotic state and gas mixing are observed in the region of turbulent flow on the boundary with helium. There appears a new feature, namely, a gravitational mixing anisotropy, which becomes apparent in the jet structure of the mixing zone.

The process of transition to the turbulent stage of mixing is characterized by large variety of flows, which depend upon precisely fixed conditions of the experiment conducted. But the asymptotic turbulent stage, in consequence to its insensitivity to initial conditions, does not depend upon conditions of the experiment conducted.

It is practically impossible to realize the asymptotic stage of mixing in the experiment because of finite dimensions of the installation and the short-term acceleration action.

Therefore, for fulfilling the analysis of experimental results, it is necessary to take into account those or other theoretical considerations about the character of dependence of the studied process upon experimental conditions.

Results of our experiments for researching the development of the mixing zone are analyzed on the assumption of a quadratic law of dependence of mixing zone width upon the time, which is described in the works [6,7]. In consequence to inconsistency of the deceleration value of the interface, this analysis was conducted on the assumption of

proportionality of mixing zone width, L , to breaking distance, S , in the following relation:

$$L = \beta f(N) \cdot 2S, \quad (2.5)$$

where: β is a constant;

N is an interface gas density relation.

The influence of initial perturbations of interface upon mixing zone dimensions was taken into consideration during processing experimental data in the coordinate plane $(\sqrt{L}, \sqrt{2S})$ proceeding from the dependence, proposed in [8],

$$\sqrt{L} = \sqrt{L_0} + \sqrt{\hat{L}}, \quad (2.6)$$

where: L_0 is the initial turbulent mixing zone width;

\hat{L} is the transient width of the mixing zone.

The concept of mixing intensity is introduced for describing the process of the gravitational turbulent mixing:

$$J = \frac{dL}{d2S} \quad (2.7)$$

Data processing was conducted on the assumption, that the value of each uncontrolled perturbation of a flow is a random value in that sense, that the combined ensemble of flow perturbations, which have statistical influence on the experiment, are realized during each controlled experiment.

Therefore data processing results, obtained in different experiments, were averaged and the average of them was adapted as the most probable outcome.

Dependence of \sqrt{L} on $\sqrt{2S}$ (see Fig. 2.5 - 2.7) has a linear form not only for the combined data of each separate experiment, but for all experiments as a whole. At $S \geq 10$ mm, this corresponds to measurements at $\hat{t} > 150 \mu s$. The average correlation coefficient is $R(\sqrt{L}, \sqrt{2S}) = 0.996$.

The transition to the linear dependence is more clearly observed for the largest perturbations ($\alpha_0/\lambda = 0.05$). This is connected apparently with

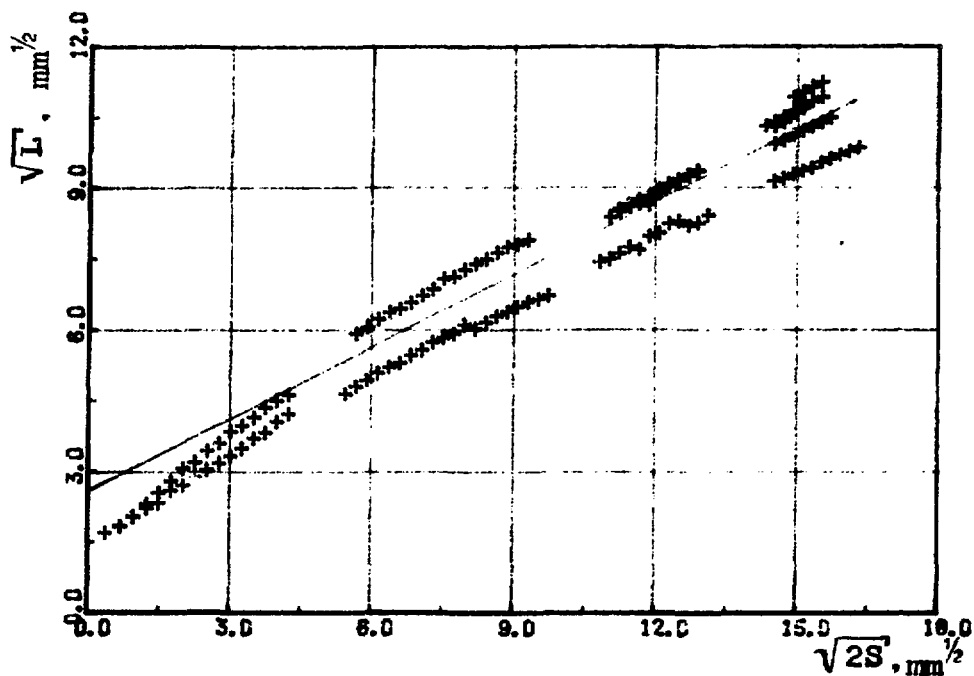


Fig. 2.5 The development of the gas mixing zone width versus braking distance in the turbulent stage. + - experimental results with the initial perturbation $\alpha_0 = 1.0$ mm, $\lambda = 25$ mm; - - the results of processing experimental dates by the method of least squares. $J = 0.26$, $L_0 = 6.7$ mm.

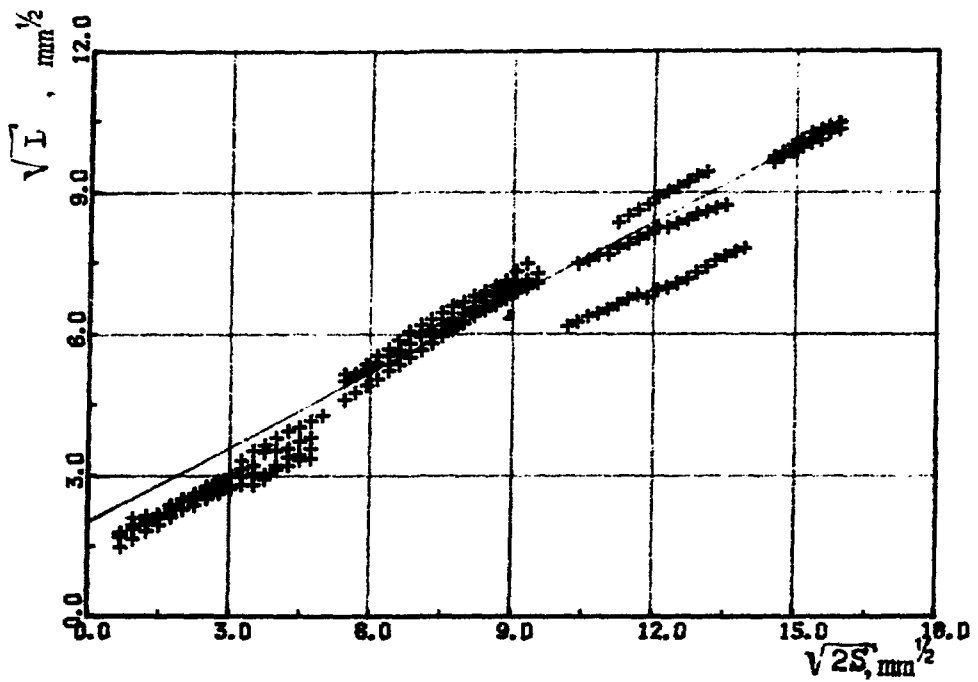


Fig. 2.6 The development of the gases mixing zone width versus braking distance in the turbulent stage. + - experimental results with the initial perturbation $\alpha_0 = 1.0 \text{ mm}$, $\lambda = 50 \text{ mm}$; - - the result of processing experimental dates by the method of least squares. $J = 0.28$, $L_0 = 4.05 \text{ mm}$.

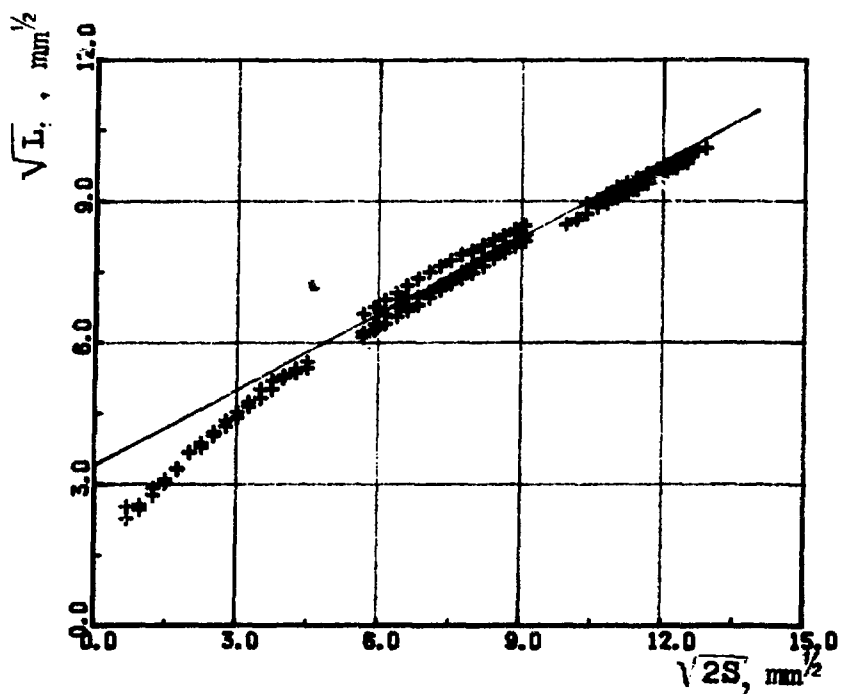


Fig. 2.7 The development of the gases mixing zone width versus braking distance in the turbulent stage. + - experimental results with the initial perturbation $\alpha_0 = 2.5$ mm, $\lambda = 50$ mm. - - the result of processing experimental dates by the method of least squares. $J = 0.29$, $L_0 = 11.6$ mm.

the decreasing significance of uncontrollable perturbations and increasing dominance of periodic distortions of the interface.

When the initial sinusoidal perturbation amplitude is decreasing, the whole mixing zone width is also decreasing, but the intensity of mixing (see Table 2.1) remains constant. It is observed that the proportionality of the relative roughness of interface α_0/λ with the effective initial mixing zone width L_0 demonstrates effectiveness of this method of experimental result processing.

The "ignoring" of initial conditions in the given case is revealed in the relation that the value of J remains constant in spite of the fact that the whole acceleration, which is acted on the interface, depends appreciably on the character of the shock wave action:

$$g(t) = U_0 \delta(t) - \hat{g} \tag{2.8}$$

where: $\delta(t)$ - Dirac's function and
 \hat{g} - acceleration, which is created by the unloading wave

TABLE 2.1
 Statistical processing results of experimental data

Series of Experiments	Number of Experiments	α_0/λ	J	ΔJ	L_0
1	8	0.02	0.28	0.04	4.05
2	6	0.04	0.26	0.02	6.70 ± 1
3	10	0.05	0.29	0.01	11.60

Data spread ΔJ is given with confidence probability $P = 0.95$.

Mixing intensity constancy, at sufficiently large changes in initial perturbations of interface, can be interpreted as establishing the turbulent stage of mixing. The observation, that the periodic structure of initial perturbations have not been destroyed at the end, is connected

apparently, with establishment of certain large-scale, periodic mixing features, which are characteristic of this phenomenon.

An additional argument in favor of such a supposition is the agreement of mixing intensity data with the results of numerical computations, which simulate the development of turbulent mixing of fluids for the case of full width of the mixing zone [9], while using two-dimensional methods.

Experimental data allow determination of the empirical constant of the gravitational turbulent mixing " β " in the dependence, as suggested in the work [7].

$$L = \beta \frac{\rho_2 - \rho_1}{\rho_2 + \rho_1} \cdot 2S, \quad (2.9)$$

where: $\beta = 0.32 \pm 0.010$.

The error of measuring the value of " β " has a confidence probability of 0.95.

It must be noted that in experiments conducted with fluids [14,16], one can observe a mixing intensity which is less by approximately a factor of two. Such a discrepancy of results cannot be completely explained by essential compressibility of the media based on data from experiments with gases.

It is possible that forces of surface tension exert a certain influence upon the development process of turbulent mixing of liquid media that, in its turn, can result in capillary instability of jets, whereas this factor is fully excluded in experiments with gases.

REFERENCES

1. Taylor, G., Proc. Roy. Soc. Ser. A, 1950, Vol. 201, N 1065, p. 192-196.
2. Lewis D., Proc. Roy. Soc. Ser. A, 1950, Vol. 202, p. 81-96.
3. Ratafia, M., Phys. Fluids, 1973, Vol. 16, N 8, p. 1207-1210.

4. Meshkov, E. E., "Some Experimental Research Results of Gravitational Instability of Interfaces of Media with Different Densities", Preprint. Keldish Inst. Appl. Math., Ac. Sci. USSR, 1981.
5. Emmons, H. W., Journ. Fluid Mech., 1960, Vol. 7, Part 2, p. 177-193.
6. Belyenkii, S. Z., Fradkin, E. S., "Theory of Turbulent Mixing Transact.", Phys. Inst. Ac. Sci. by name of Lebedev, Vol. 29, p. 207-238, 1965.
7. Neuvazhaev, V. E., "To the Theory of Turbulent Mixing", Rep. Ac. Sci. USSR. 1975, Vol. 222, N 5, p. 1053-1056.
8. Neuvazhaev, V. E., Yakovlev, V. G., "About Mixing of Interface Decelerated by Stationary Shock Waves", J. Appl. Mech. and Tech. Phys., 1981, p. 85-89.
9. Andronov, V. A., Bahrah, S. M., et al., "Numerical Simulation of Some Turbulent Flows in Approximation to Two-Dimensional Turbulence", Proc. Ac. Sci. USSR, Fluid Mech., N 6, 1984, p. 20-27.
10. Anuchina, N. N., Ogibina, V. N., "Numerical Research of Gravitational Instability of Interface of Media with Different Densities", Physical Mechanics of Nonuniform Media Trans. Edited by T. V. Gadizak. Ac. Sci. USSR, Sib. Dept., Inst. Teor. and Appl. Mech., Novosibirsk, 1984.
11. Anuchina, N. N., Ogibina, V. N., "Computerized of Hydrodynamic Instability Transact.", edited by Babenko, K. J., Keldish Inst. Appl. Math., Ac. Sci., USSR, Moscow, 1981.
12. Neuvazhaev, V. E., "Model Characteristics of Turbulent Mixing of Interface of Accelerated Fluids with Different Densities", J. Appl. Mech. and Tech. Phys., 1983, N 5, p. 81.
13. Neuvazhaev, V. E., "Diffusion of Mixture Turbulent Layer", J. Appl. Mech. and Tech. Phys., 1988, N 2, p. 46.
14. Anuchina, N. N., Kucherenko, Y. A., Neuvazhaev, V. E., et al., "Turbulent Mixing on Accelerating Interface of Fluids Having Different Densities", Proc. Ac. Sci. USSR, Fluid Mech., 1978, N 6, p. 157-160.
15. Andronov, V. A., Bahrah, S. M. et al., "Turbulent Mixing on the Contact Surface, Accelerated by Shock Waves", J. Exp. and Ther. Phys., 1976, N 7 (Issue 218).

16. Read K. J., *Physica*, 1984, p. 45-58.
17. Makarov, Y. V., Chekalin, E. K., "Physical Processes in Electromagnetic Tube.", Atomisdat, 1986.
18. Buzhinskii, O. I., Volkov, L. P., "Investigation of Shock Waves Excited in Electromagnetic Shock Tube.", *J. Tech. Phys.*, 1972, Vol. 42.
19. Keck, J., *Phys. of Fluids*, 1964, 7, N 11, p. 186-197.
20. Zeldovich, Y. B., Raizer, Y. P., "Physics of Shock Waves and High-Temperature Hydrodynamic Phenomena", Academic Press, New York, 1967.
21. Kuropatenko, V. F., Potapkin, B. K., "Experience of Creating Large Programs of Serial Count after the Example of the Program 'RAND'", Complexes of Mathematical Physics Programs, Trans. Novosibirsk, 1972.
22. Kay, J., Laby, T., "Tables of Physical and Chemical Constants", Publishing House "Nauka" (Phys. Math.), 1962.
23. Meyer, K. A., Blewett, P., *Phys. Fluids*, 1972, Vol. 15, N 5, p. 753-759.
24. Richtmyer, R. D., *Comm. Pure and Appl. Math.*, 1960, Vol. 13, N 2, p. 297-319.
25. "Turbulence Principles and Applications", Edited by Frost, U., Mowlden, T., Moscow, "MIR," 1980, p. 9-32.